The Morphology and Structure of Post-Braze Flux Residues

A. Gray‡, H.-W. Swidersky∗, D. C. Lauzon+

‡Alcan International Ltd. (UK), ∗Solvay Fluor und Derivate GmbH (Germany), +Solvay Fluorides, Inc. (USA)

ABSTRACT

Since the early 1980's, NOCOLOK® Flux brazing – or Controlled Atmosphere Brazing (CAB) with non-corrosive fluxes – has been the preferred process for manufacturing aluminum automotive heat exchangers.*

Earlier work showed that at excessively high flux loads the level of corrosion resistance exhibited by the residual flux layer was reduced. No explanation was provided for this reduction in corrosion resistance.

This current work attempts to identify the specific parameters responsible for this effect, namely surface topography, coating integrity, and flux adhesion. The variables were investigated with respect to flux load (1 – 20 g m^{-2}) and alloy composition. This is part of ongoing research, and for this phase of the work the focus was on standard braze conditions, however, it is recognized that these braze conditions could have a marked effect on both morphology and structure of the flux residue.

Initial results indicate that the surface roughness (R_a) of the residual layer reaches a plateau at approximately 10g/m^2. This suggests that the reduction in corrosion resistance beyond 20g/m^2 as observed in the earlier work is not solely attributable to surface roughness.

For this work, the residual flux layer was characterized using conventional SEM and 3D surface imaging techniques. In addition to these, we have also attempted to characterize the integrity of the layer using a combination of microtoming and TEM methods.

The objective of this work is to provide a fundamental characterization of the flux residue layer.

1.0 Introduction

When the NOCOLOK brazing process was first introduced, typical flux usage for radiator applications was between 12 and 15 g m^{-2}. However, it is now more common to run between 2 and 5 g m^{-2} as the drive to minimize flux levels continues in the ever increasing efforts of the various the Heat Exchanger Manufacturers to support their cost-down activities. Indeed, it is known that for some applications Japanese Manufacturers are running at flux levels below 2 g m^{-2}.

But this trend of reducing flux usage does raise the question of the impact on air-side corrosion resistance of radiator products. Early workers [1,2] in this area recognized that the post-brazed residual flux layer did give measurable improvements in corrosion resistance when using AA3003-based core alloys. However, Takigawa and his co-workers[3] have reported increased pitting susceptibility in 3003/4045 material following CASS [4] testing for 250 and 500 hrs.

More recently [5], Gray *et al* demonstrated similar effects with non long-life alloys (AA3003) when flux levels were allowed to increase towards 20 g m^{-2}. However, at that time the precise mechanism behind the reduction in corrosion resistance remained unclear.

* NOCOLOK is a registered trademark of SOLVAY Fluor und Derivate GmbH

2.0 Experimental

2.1 Materials

All of the materials used in this current study were commercially rolled clad/core packages manufactured at Alcan's sheet rolling facility in South Wales, UK. The chemical analyses of the core alloys are noted in Table 1 and were determined by Optical Emission Spectroscopy (OES).

Alloy packages are designated as follows:

- X314 = 3003 core clad with AA4343
- X907 = X900 core clad with AA4045

Table 1 Chemical Composition of Core Alloys

Alloy	Chemical analysis (wt%)					
	Si	Fe	Mn	Cu	Mg	Zn
X314	0.21	0.55	1.05	0.14	0.10	<0.02
X907	0.05	0.11	1.46	0.58	0.26	<0.02

2.2 Fluxing and Brazing Conditions

Various flux types, including standard NOCOLOK® Flux, NOCOLOK® Cs Flux (from Solvay Fluor und Derivate) and a competitor non-corrosive flux were used in this investigation. The fluxes were applied at various levels between 1 and 20 g m^{-2} to coupons 25 mm x 25 mm and brazed under the following conditions:

- Heating rate 20 °C min^{-1}
- Peak temperature 600 °C
- Dwell time at peak 5 min.
- Cooling rate 30 °C min^{-1}

2.3 Flux Residue Characterization

Surface topography of the residual flux layers was quantified using a 3-D scanning interference microscope (Wyko NT 2000). This non-contact method generates 3-dimensional images of surfaces to a depth of 500 μm with a spatial resolution from 0.1 nm to several mm by vertically scanning the surface. For this exercise the parameters measured were:

- R_a arithmetic average roughness height over the entire 3D surface
- R_z difference between the average of the highest peaks and lowest valleys
- R_t vertical distance between highest peak and lowest valley

These are shown schematically in Figure 1.

The residual flux layers were characterized using conventional SEM (scanning electron microscope), EPMA (electron probe microanalysis) and TEM (transmission electron microscope) techniques. For the TEM characterization sections were produced using an ultramicrotomy method.

Ultramicrotomy (UM) is a preparation technique to produce samples for examination by transmission electron microscopy (TEM). Essentially it involves cutting thin, electron-transparent slices of material. It was initially developed as a method of preparing biological materials for

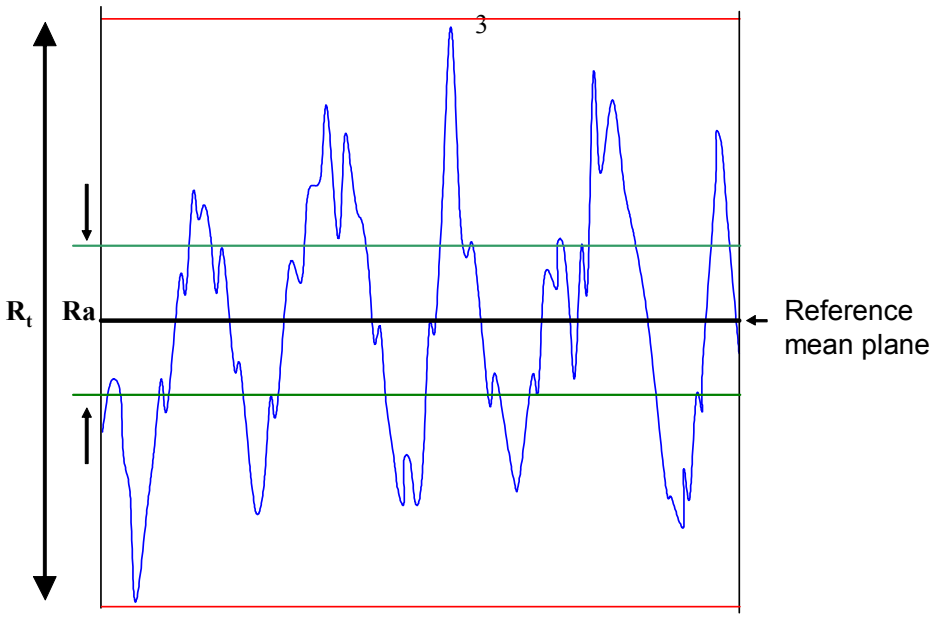

Figure 1 Schematic showing definitions of R_a and R_t

TEM, but more recently has found application for inorganic materials, particularly those that are not very electron-dense such as aluminum. Studies of aluminum have largely concerned surface films where UM enables the production of cross-sections of real material (not replicas) sufficiently thin for TEM, and alloys which are not amenable to electro-polishing preparation techniques because phases of interest are rapidly dissolved out of the matrix.

Ultramicrotomes have a chuck to hold the samples, which moves in a series of vertical strokes past a diamond knife. The knife is mounted so that a water bath is contained behind its edge (Figure.2). As slices are cut, they collect on the surface of the water, and may be subsequently removed using a TEM grid, dried and examined in the TEM. Typically, slices are 20-50nm thick but can be as thin as 7nm [6], and about 20 x 20 mm in size.

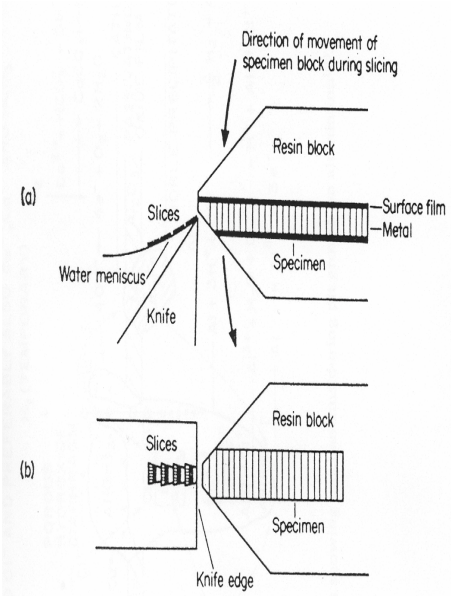

Figure 2 Schematic showing manufacture of microtomes

3.0 Results and Di

From the start of the NOCOLOK development and subsequent commercialization, had been recognized that the residual surface layer left after brazing with the non-corrosive flux imparted a degree of corrosion protection to brazed components, in particular when testing the air-side corrosion resistance of radiator units. Much of this early work was done on 3003/3105 type alloys using significantly higher flux loading than is common place in the industry today.

At the 2001 AFC-Holcroft Therm Alliance Seminar, it was shown that corrosion resistance, as measured by SWAAT, did in fact reduce when the flux levels used were below 5 g m^{-2}. However, this effect was readily overcome if X900 type alloys were used and the corrosion resistance remained stable over a wide range of flux levels (1 to 20 g m^{-2}). At very high flux levels, approximately 20 g m^{-2}, it was observed that the corrosion protection afforded by the residual flux layer began to be reduced. These results were consistent with earlier work by Yamaguchi and his colleagues who saw similar effects at equivalent flux levels but when tested using the CASS test.

In both cases, these effects were observed with 3003 type alloys. Whilst the use of flux levels beyond 10 g m^{-2} remains uncommon it is recognized that in some parts of a heat exchanger component, dependent on geometry, it is possible for flux to accumulate to give local levels approaching 20 g m^{-2}. This current study attempts to provide an understanding of why this reduction in corrosion resistance occurs and reports the first phase of our work in this area.

3.1 Flux Surface Roughness

For both of the flux types tested (non-corrosive fluoride containing and Cs addition) the surface roughness increased as the flux loading increased (Figures 3 to 5). The magnitude of this increase in R_a was similar for all the flux variants i.e. no significant influence of flux type. As the flux loading was increased from 1 to 20 g m^{-2} the magnitude of the increase in mean surface roughness was approximately X2 for the X314 material (4343 cladding) and X3 for the X907 variant (4045 cladding). This increase in surface roughness of the X907 material was particularly noticeable at the higher flux level were the R_a value was some 15% higher than that measured on the corresponding X314 sample.

The exact reason for this remains unclear but could be associated with either the difference in cladding alloy or the significant difference in core alloy grain size/composition.

In a further attempt to understand the role of the cladding alloy in any influence on the surface roughness of the residual flux layer a similar characterization (X314 only) of the surface roughness after brazing was carried out on material without the AA4343 cladding layer present.

These results are shown in Figure 6 were it can be seen that the increase in surface roughness with increasing level of flux is less marked and overall R_a values are significantly lower than those measured on the corresponding clad variants. In fact at the 1 g m^{-2} level the surface roughness is virtually identical to that of an un-fluxed sample subjected to the same braze cycle i.e. an oxidized surface only.

Figure 7 shows the changes in surface topography that occur as the flux level increases from 1 to 20 g m^{-2} for the standard NOCOLOK variant. Comparative 3D images for the different flux types are shown in Figures 8 & 9 for X314 and X907 alloys respectively. These images confirm the similarity of the residual flux surfaces within each alloy group irrespective of the flux type tested.

For comparison, the 3D surface images from the unclad X314 variant are shown in Figure 10 and clearly shows the reduction in surface roughness, where irrespective of the flux level the surface topography of the as-rolled surface of the sheet is still visible.

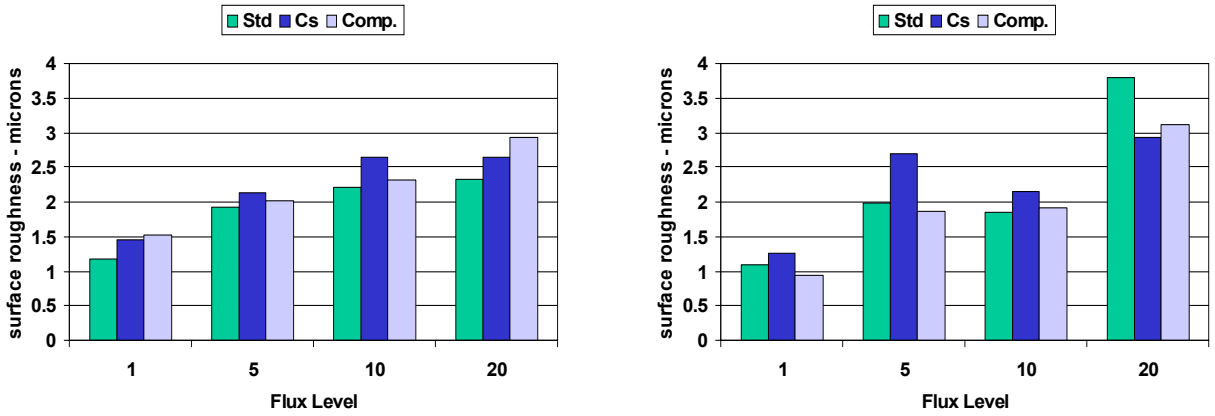

Figure 3 R_a for X314 & X907 alloys for all flux types

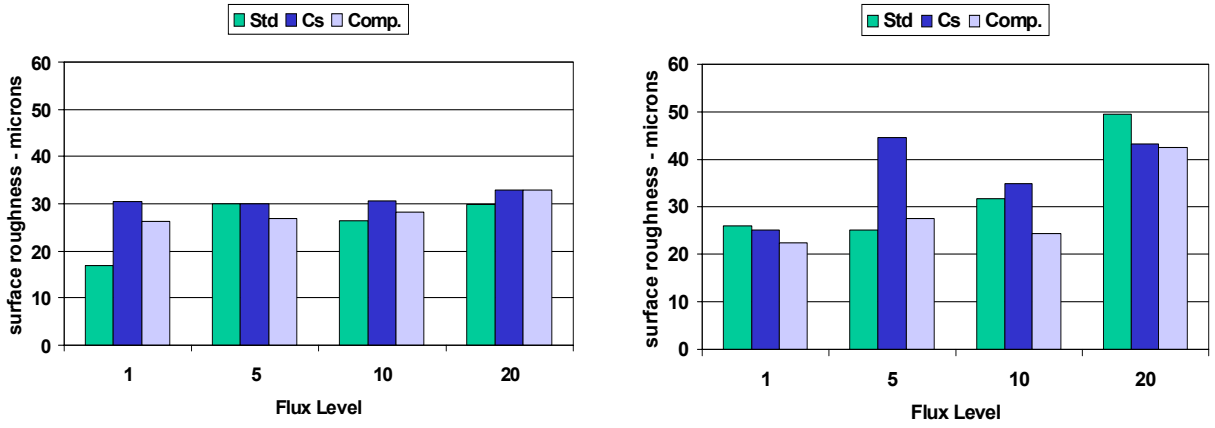

Figure 4 R_t for X314 & X907 alloys for all flux types

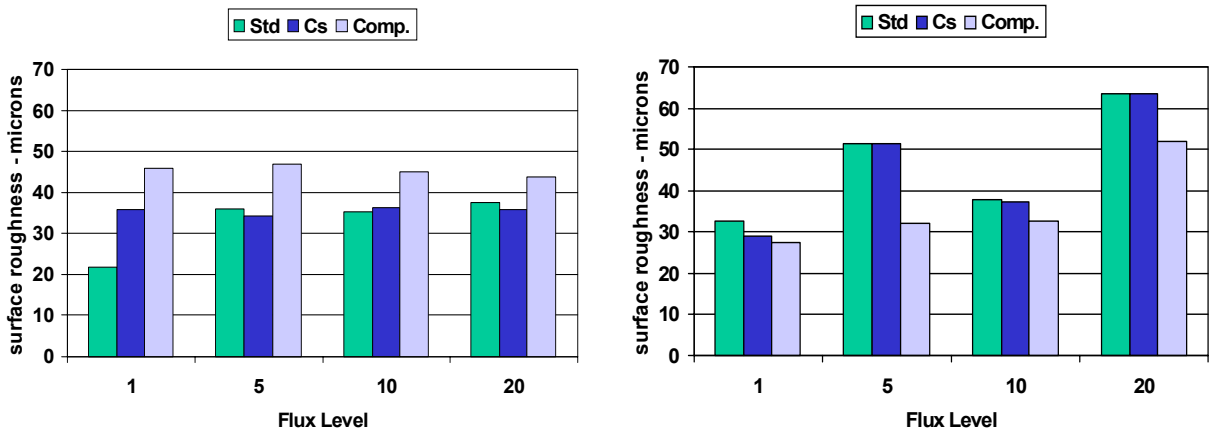

Figure 5 R_z for X314 & X907 alloys for all flux types

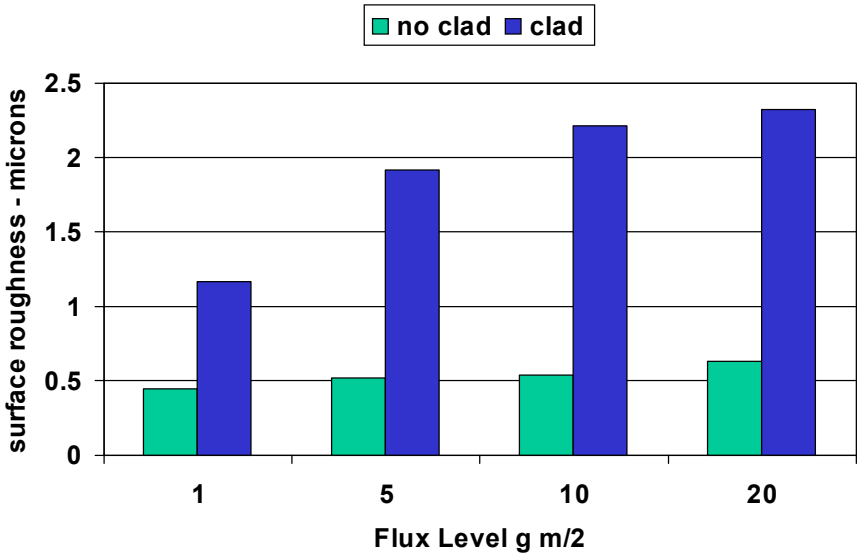

Figure 6 R_a for X314 alloy clad vs unclad

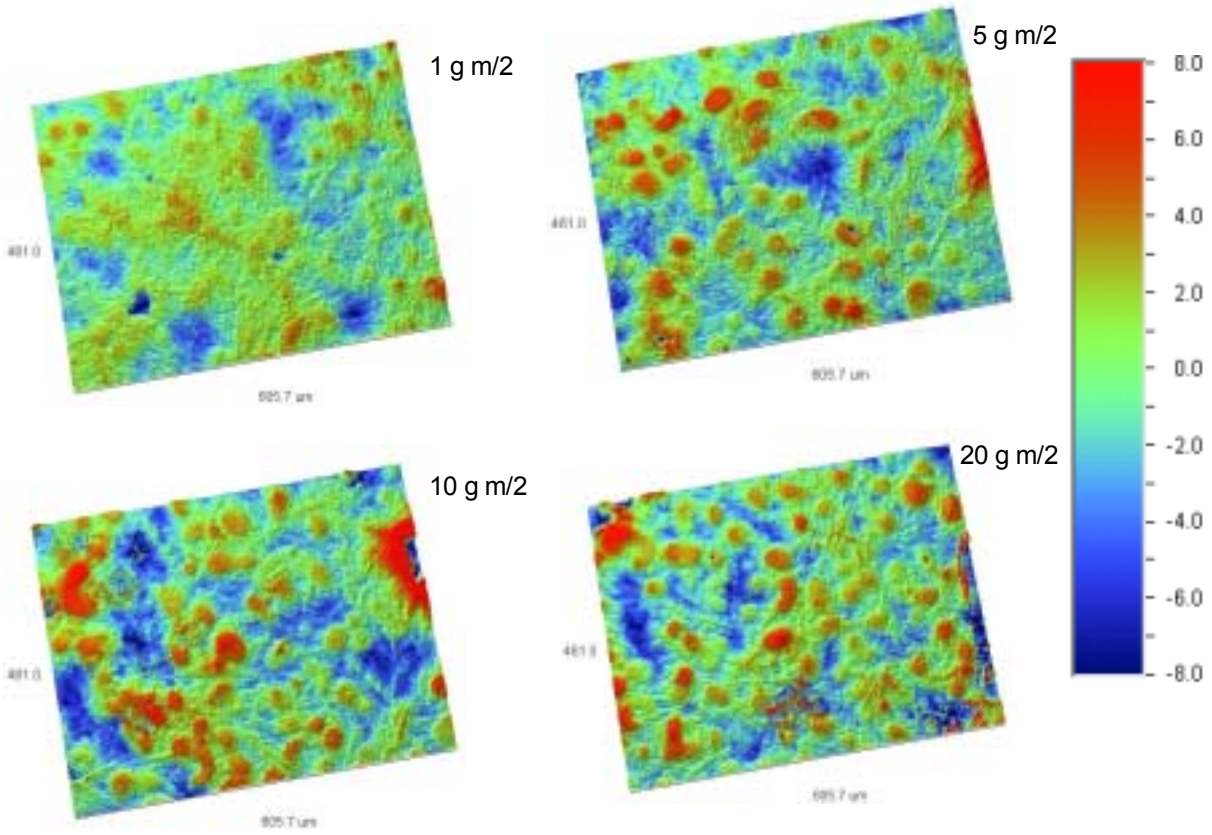

Figure 7 Wyko 3D images for different flux levels on X314

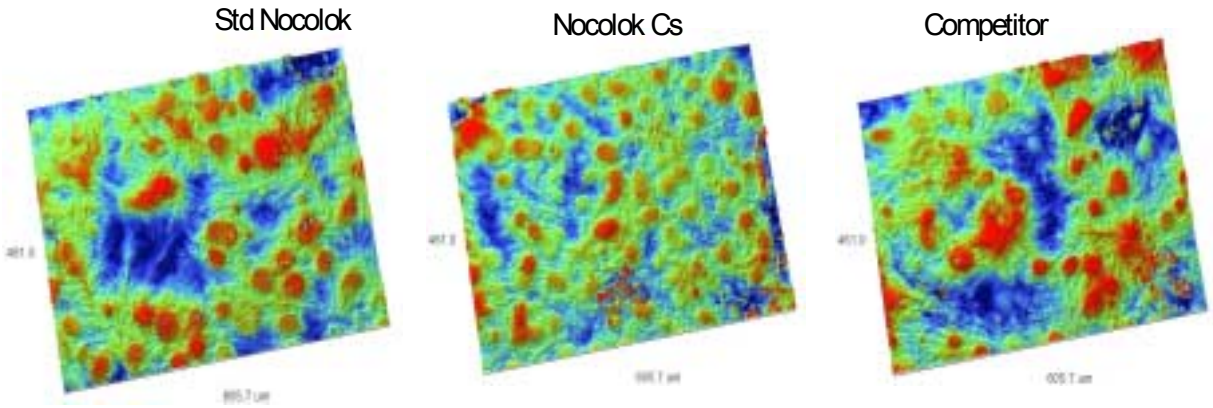

Figure 8 Wyko 3D images for X314

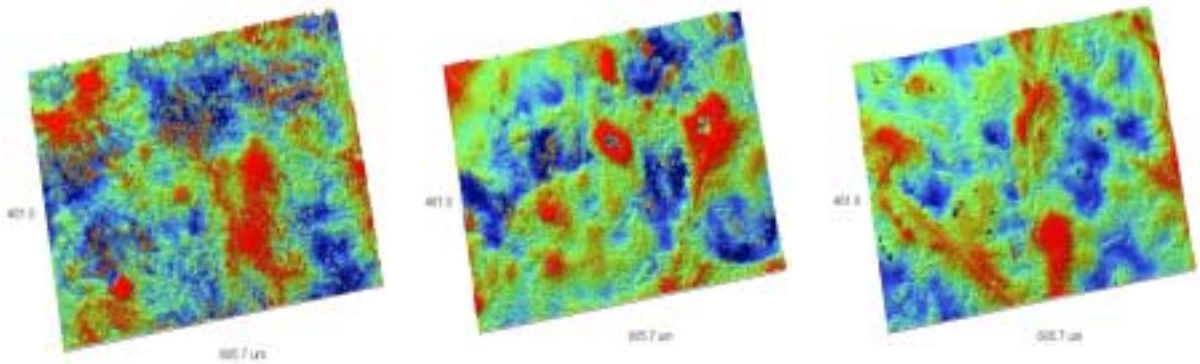

Figure 9 Wyko 3D images for X907

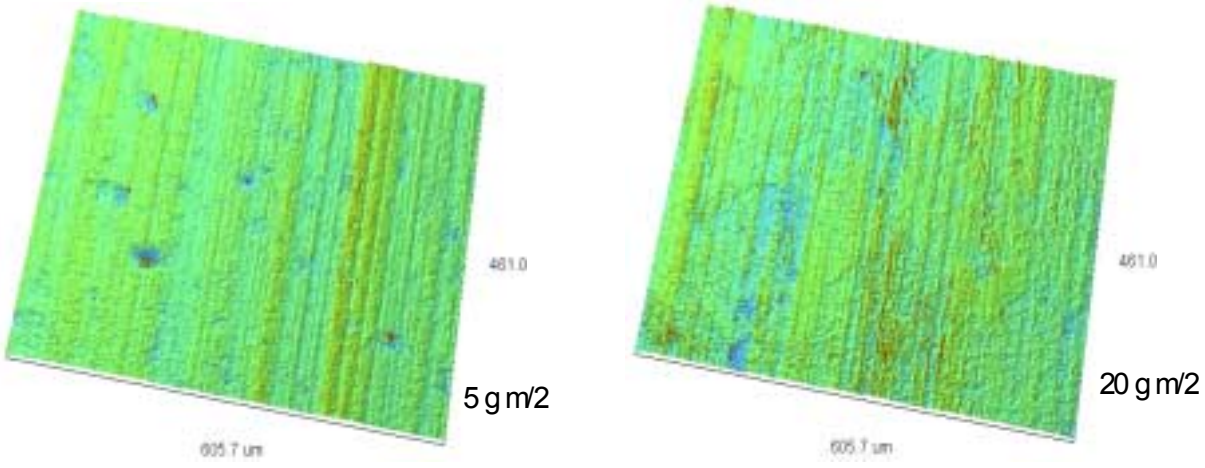

Figure 10 Wyko 3D image of unclad X314 material

3.2 Flux Morphology and Analysis

The SEM images shown in Figure 11 confirm similarity of the residual flux morphologies of the three different flux types at the 20 g m^{-2} level. One surprising feature observed on the low magnesium alloy, X314, is the significant level of the needle-like K-Mg-F phase. This highlights the affinity that the NOCOLOK flux has for magnesium as it diffuses from the core alloy during the braze cycle or the magnesium within the cladding alloy itself. It is well known that the high melting point K-Mg-F phase reduces clad fluidity of the high Mg-containing alloys.

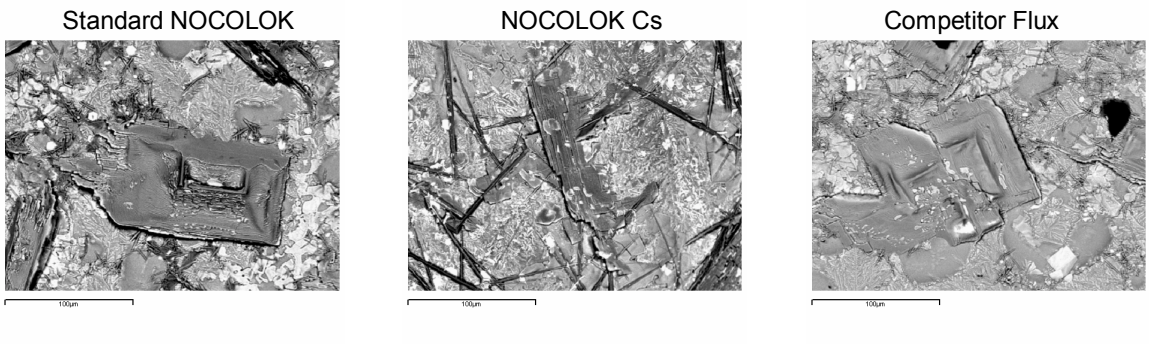

Figure 11 SEM images of residual flux surface - 20 g m/2 level

One interesting feature of the residual flux layer on the unclad 3003 alloy is the complete absence of the K-Mg-F needle-like phase and the increasing size and therefore coverage, of the K-Al-F platelets as the flux level increases, Figure 12.

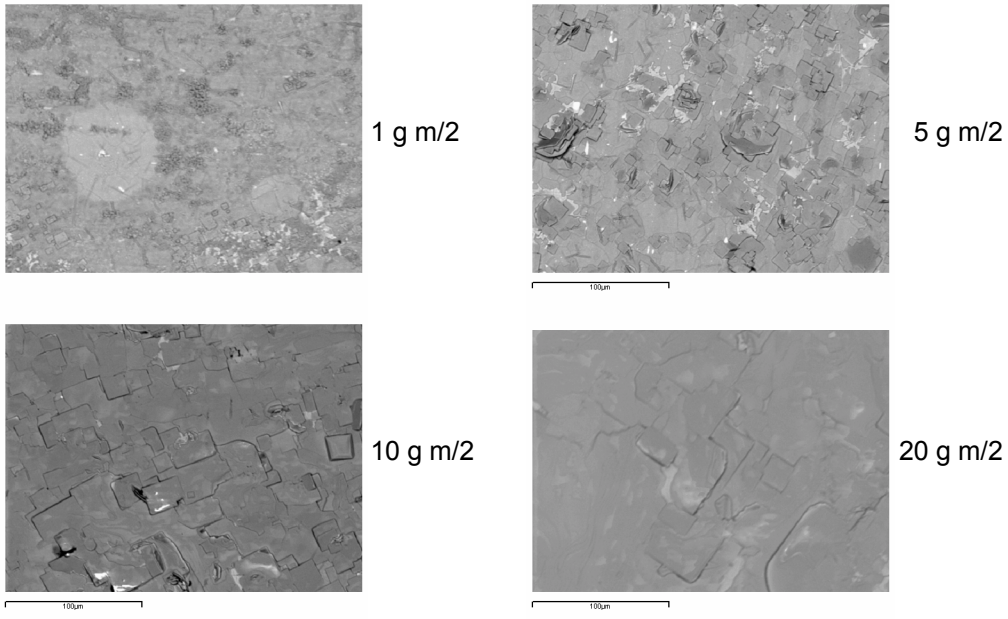

Figure 12 SEM images of residual flux surfaces on unclad X314

In addition, to the SEM imaging/analysis, residual flux layers were also analyzed using an EPMA technique. This has the advantage of improved resolution and a WDX (wavelength dispersive X-ray analysis) capability. Figure 13 shows the analysis of the NOCOLOK-Cs flux at the 20 g m^{-2} level.

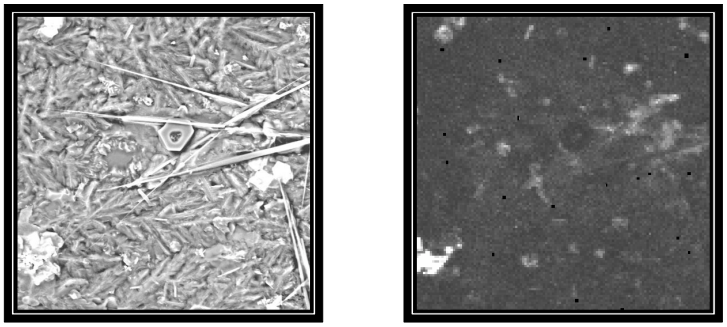

Figure 13 EPMA element mapping showing cesium in Nocolok Cs flux

Microtomed sections through the residual flux layer (Figure 14) clearly show a duplex structure; an extended pore-like structure at the metal/flux interface with a more amorphous-like layer at the surface. However, from the SEM/EPMA analysis we know this is a multi-phase layer which has been confirmed by removing flux residues from the coupon surface and analyzing using an X-ray diffraction method (XRD). Results from the 20 g m^{-2} variant of each alloy system are noted in Table 2.

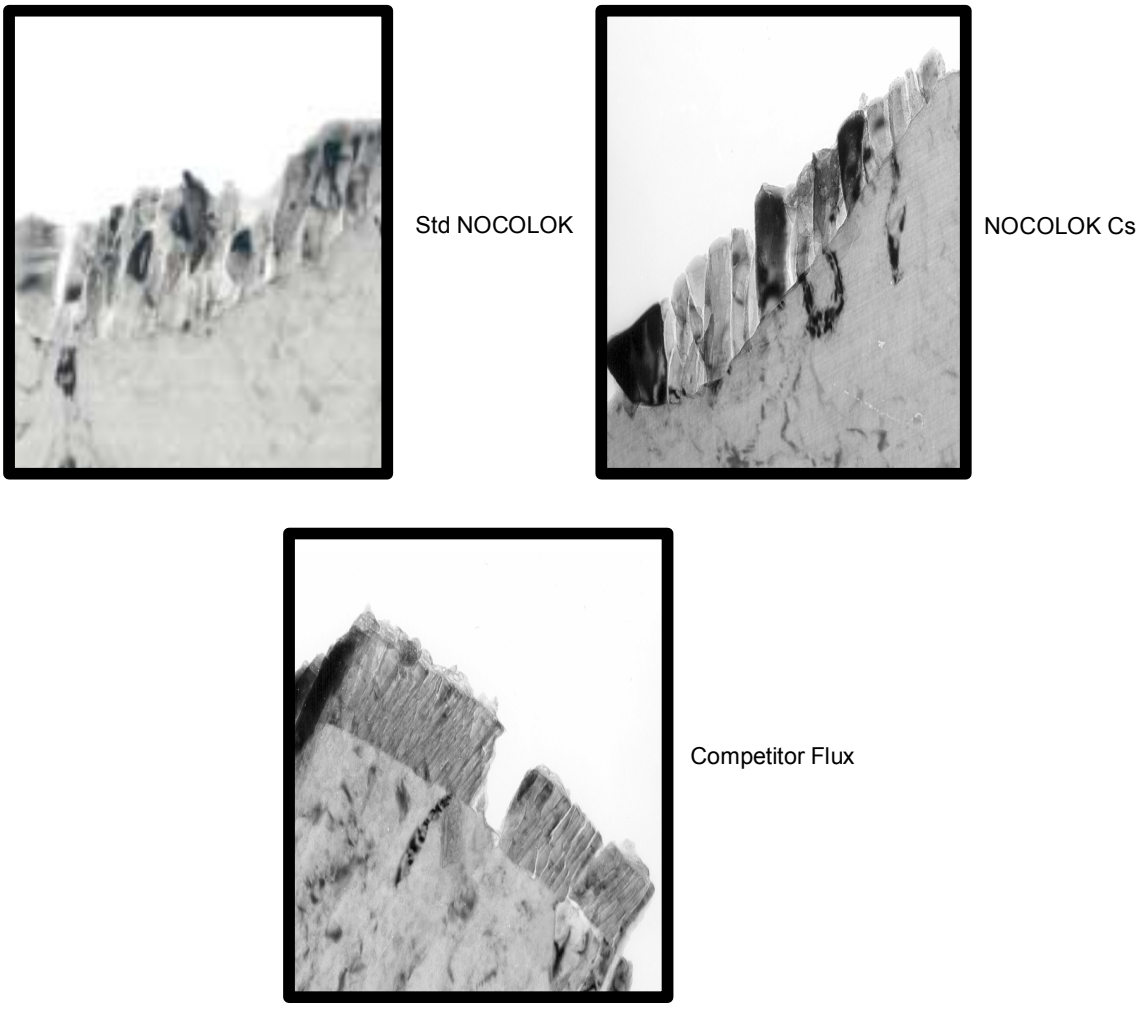

Figure 14 Microtomed sections through residual flux layer

Table 2 X-ray Diffraction Results

Alloy	Phases identified
X314(clad)	**$KAlF_4$, K_3AlF_6,** $MgAl_2O_4$, K_2MgF_4
X914	**$KAlF_4$, K_3AlF_6,** $MgAl_2O_4$, **K_2MgF_4**

Note: phases in **bold** are the predominant phases present

4.0 Summary

In what are commonly referred to as low magnesium alloys (Mg < 0.05 wt%) the high melting point K-Mg-F phases are readily formed even at low levels of flux – 1g m^2. In the present study, it is likely that it is the cladding alloy is the source of the magnesium for the X314 variant.

As the flux loading is increased from 1 to 20 g m^{-2} there is a progressive increase in the surface roughness, R_a, of the residual flux layer from approximately 1.5 μm to between 3 and 3.8 μm for both the X314 and X907 materials.

These trends in surface roughness were similar for the standard NOCOLOK, NOCOLOK Cs and competitor flux.

For the same range of flux loading this increase in surface roughness is much reduced for the unclad 3003 alloy.

Characterization of the residual flux layer using a combination of EPMA and microtoming did reveal the presence of micro flaws which in an earlier study had appeared to dominate behavior in a range of electrochemical tests used to try and provide a better quantification of corrosion behavior than the commonly employed salt spray tests.

The use of the microtoming technique to 'visualize' the internal structure of the residual flux layer appears to provide a powerful tool for characterization of the integrity of this layer.

Whilst it is has been shown in earlier work, that with extended corrosion testing that the flux loading does influence the corrosion performance of brazing sheet materials based on 3003 type alloy. The findings of the present study suggest that is effect is unlikely to be directly linked to just the surface roughness increase.

5.0 Conclusions

1. There is a progressive increase in surface roughness of the residual flux layer as flux levels are increased to 20 g m^{-2}.
2. This increase in surface roughness is greatly reduced if the substrate is 3003 alloy rather than the low melting point Al-Si alloy.
3. It is probable that the presence of the K-Mg-F phase in the residual flux layer on the X314 composite is associated with the magnesium in the 4343 cladding alloy rather than the 3003 core material.
4. The residual flux layer is comprised of two distinct layers; a pore-like layer adjacent to the metal surface and a thinner multi-phase layer at the flux/air interface.
5. It is unlikely that the reduction in corrosion resistance seen at high flux levels is associated with the increase in the surface roughness of the residual flux layer.

6.0 Acknowledgements

The authors would like to express their gratitude to Thomas Born of Solvay Fluor und Derivate for his assistance with the preparation of the brazed coupons. Also, Karen Hall, Alice Banks and Ann Stoker with the testing and characterization and to Alcan International Limited and Solvay Fluor und Derivate, for permission to publish this paper.

7.0 References

1) Claydon et al. Brazing Aluminium Automotive Heat Exchanger Assemblies Using A Non-Corrosive Flux Process. SAE 830021, 1983

2) Ando et al. Development of Aluminium Radiators using the NOCOLOK Brazing Process – Corrosion Resistance of New Aluminium Radiators by Applying a NOCOLOK Brazing Process. SAE 870180, 1987

3) Takigawa et al. Materials and Process Factors in Non-Corrosive Flux Brazing for Aluminium Automobile Heat Exchangers. Kobelco Technology Review, No. 16 April 1993

4) ASTM B368 Method for Copper Accelerated Acetic Acid Salt Spray (fog) Testing (CASS Test)

5) Gray, A. & Afseth, A. 2nd Aluminium Congress on Aluminium Brazing, Düsseldorf, May 2002

6) Malis, T.F & Steele, D. Mat.Res. Symp. Proc., Vol. 199 (1990)